Published in final edited form as:
Cancer Res. 2014 June 1; 74(11): 3146–3156. doi:10.1158/0008-5472.CAN-13-3728.

Failure to induce apoptosis via BCL-2 family proteins underlies lack of efficacy of combined MEK and PI3K inhibitors for KRAS mutant lung cancers

Aaron N. Hata[1,2], **Alan Yeo**[1], **Anthony C. Faber**[1], **Eugene Lifshits**[1], **Zhao Chen**[3,2], **Katherine A. Cheng**[3], **Zandra Walton**[3], **Kristopher A. Sarosiek**[3], **Anthony Letai**[3], **Rebecca S. Heist**[1,2], **Mari Mino-Kenudson**[4], **Kwok-Kin Wong**[3,2], and **Jeffrey A. Engelman**[1,2]

[1]Massachusetts General Hospital Cancer Center, Charlestown, MA 02129, USA

[2]Department of Medicine, Harvard Medical School, Boston, MA 02115, USA

[3]Department of Medical Oncology, Dana-Farber Cancer Institute, Boston, MA 02115, USA

[4]Department of Pathology, Massachusetts General Hospital, Boston, MA 02115, USA.

Abstract

Although several groups have demonstrated that concomitant use of MEK and PI3K inhibitors (MEKi/PI3Ki) can induce dramatic tumor regressions in mouse models of *KRAS* mutant non-small cell lung cancer (NSCLC), ongoing clinical trials investigating this strategy have been underwhelming to date. While efficacy may be hampered by a narrow therapeutic index, the contribution of biological heterogeneity in the response of *KRAS* mutant NSCLCs to MEKi/PI3Ki has been largely unexplored. In this study, we find that most human *KRAS* mutant NSCLC cell lines fail to undergo marked apoptosis in response to MEKi/PI3Ki, which is key for tumor responsiveness in vivo. This heterogeneity of apoptotic response occurs despite relatively uniform induction of growth arrest. Using a targeted shRNA screen of BCL-2 family members, we identify BIM, PUMA and BCL-XL as key regulators of the apoptotic response induced by MEKi/PI3Ki, with decreased expression of BIM and PUMA relative to BCL-XL in cell lines with intrinsic resistance. Additionally, by modeling adaptive resistance to MEKi/PI3Ki both in vitro and in vivo, we find that, upon the development of resistance, tumors have a diminished apoptotic response due to down-regulation of BIM and PUMA. These results suggest that the inability to induce apoptosis may limit the effectiveness of MEKi/PI3Ki for *KRAS* mutant NSCLC by contributing to intrinsic and adaptive resistance to this therapy.

Keywords

KRAS; MEK; PI3K; lung cancer; apoptosis

Address correspondence to: Jeffrey A. Engelman, Massachusetts General Hospital Cancer Center, 149 13th St, Charlestown, Massachusetts 02129, USA. Phone: 617.724.7298; Fax: 617.724.9648; jengelman@partners.org..

Conflict of Interest: J. Engelman - Novartis (sponsored research and consulting), Astra Zeneca (sponsored research and consulting), Genentech (consulting), GlaxoSmithKline (consulting); A. Letai - Abbvie (consulting).

Author contributions: ANH, AY, EL, ZC, KAC, ZW, KAS performed the experiments. ANH, ACF, ZC, KAS, JAE designed the experiments and analyzed the data. AL, RSH, MMK, KKW provided key reagents and expertise. ANH and JAE wrote the manuscript.

Introduction

Advances in the understanding of genetic alterations in non-small cell lung cancer (NSCLC) have given rise to therapies that target specific oncogenic signaling pathways. For example, cancers that harbor activating *EGFR* mutations or the *EML4-ALK* translocation are highly sensitive to the EGFR inhibitors erlotinib and gefitinib or the ALK/MET inhibitor crizotinib, respectively, with response rates of approximately 60-70% (1-3). However, no highly effective therapies have been developed for cancers harboring mutant *KRAS*, which account for 20-25% of NSCLC as well as a 35-45% of colon cancers and 80-95% of pancreatic cancers. Thus there continues to be a great need for new therapeutic strategies for *KRAS* mutant cancers.

Activating mutations in KRAS lead to impaired GTPase activity and constitutive activation of multiple signaling pathways that regulate growth and survival, including RAF/MEK/ERK, RalGDS, and in some instances, PI3K/AKT (4). While attempts to directly target the mutant KRAS protein have so far proven unsuccessful, an alternative approach is to target these downstream signaling pathways in combination. Several groups have demonstrated that dual inhibition of MEK and PI3K leads to tumor regression in experimental models of *KRAS* mutant cancers (5-8). This has spurred the rapid clinical development of this combination for *KRAS* mutant cancers, and although responses have been noted, the emerging data have been underwhelming to date (9-12). Although the tolerability of this combination when administered daily remains questionable, it is also not clear what proportion of *KRAS* mutant NSCLCs are even truly sensitive to combined MEKi/PI3Ki, and the molecular features that underlie sensitivity to this therapy have not been defined.

In cancers driven by receptor tyrosine kinases (RTKs) such as EGFR and ALK, inhibition of the corresponding RTK leads to suppression of the MEK and PI3K pathways, resulting in cell cycle arrest and apoptosis (13). Induction of apoptosis is critical for tumor regressions in vivo, and a diminished apoptotic response contributes to intrinsic resistance to EGFR inhibitors in *EGFR* mutant NSCLC (14, 15). These signaling pathways modulate the BCL-2 family of proand anti-apoptotic proteins that regulate the mitochondrial apoptotic response. For instance, ERK-mediated phosphorylation of the pro-apoptotic BCL-2 family member BIM leads to its proteasomal degradation (16), and suppression of ERK signaling results in increased BIM protein levels, which is key for response to tyrosine kinase inhibitors (13, 17-19). Furthermore, in some instances, targeted therapies may impact the expression of anti-apoptotic mediators such as BCL-XL and MCL-1 by their effects on the NF-kappaB and TORC1, respectively (13, 20). Thus, altering the balance of pro- and anti-apoptotic mediators by suppression of activated kinase signaling pathways is a critical component of effective targeted therapies.

In this study, we investigated the response of human *KRAS* mutant NSCLC to MEKi/PI3Ki. Using a collection of human *KRAS* mutant NSCLC cell lines, we observed that the majority had impaired responsiveness to MEKi/PI3Ki, resulting from the differential ability of MEKi/PI3Ki to induce a robust apoptotic response. Furthermore, loss of the apoptotic response was associated with the development of resistance to MEKi/PI3Ki in vitro and in

vivo. These results provide insight into the molecular mechanisms underlying sensitivity and resistance of *KRAS* mutant NSCLC to MEKi/PI3Ki therapy.

Materials and Methods

Cell lines and reagents

Human *KRAS* mutant and *EGFR* mutant NSLCLC cell lines were obtained from the Center for Molecular Therapeutics at the MGH Cancer Center which performs routine SNP and STR authentication (21); cell lines were passaged for less than 6 months following receipt. A427-R and DV-90-R resistant cell lines were generated by exposing parental cell lines to 1 μM AZD6244/GDC-0941 for three days followed by drug washout for 3 days. Cells were treated for 5-10 cycles, followed by maintenance in the continuous presence of drug. The N1, N2 (treatment naïve) and R1, R2, R3 (AZD6244/BEZ235 resistant) lines are tumor-derived cell lines from *Kras* $p53^{L/L}$ mice. For cell culture studies, AZD6244 (Otava), GDC-0941 (Chemietek), ABT-263 (Active Biochem), ABT-199 (Active Biochem), NVP-BEZ235 (kindly provided by Novartis) were dissolved in DMSO to a final concentration of 10 mmol/l and stored at −20°C. Antibodies utilized for western blotting are listed in Supplementary Materials and Methods.

Cell proliferation analysis

Cell lines were seeded 24 hours before addition of drug. Cells were treated with drugs for 72 hours or as indicated and proliferation determined by CellTiter-Glo assay (Promega). For time course experiments, multiple identical plates were seeded and at indicated time points were frozen at −80°C. All plates were then developed at the end of the experiment simultaneously.

Annexin/PI staining by flow cytometry

Cells were seeded at low density 24 hours prior to drug addition. After 72 hours floating and adherent cells were collected and stained with propidium iodide and Cy5-Annexin V and analyzed by flow cytometry. % apoptotic cells was calculated by subtracting percentage of annexin positive cells in vehicle control from percentage of annexin positive cells with drug treatment.

shRNA screen

Bacterial pLKO shRNA clones (4-10 per gene) were obtained from the Molecular Phenotyping Laboratory at MGH. Lentiviral stocks were produced according to the RNAi Consortium protocol from the Broad Institute. Protein knockdown efficiency was determined by western blotting using A549 cells, and hairpins with the best knockdown were selected for use (Table S2). Cell lines were infected with lentivirus in an arrayed 96-well format at viral concentrations 2-3x MOI. After 24 hours, the virus was removed and cells were cultured for 48 hours in normal media. Cells were then treated with 1 μM AZD6244/GDC-0941 for 48 hours and cell viability and caspase 3/7 activity were determined ApoTox-Glo assay (Promega).

Mouse treatment studies

All mouse studies were conducted through Institutional Animal Care and Use Committee–approved animal protocols in accordance with institutional guidelines. For xenograft studies, cell line suspensions were prepared in 1:10 matrigel and 5×10^6 cells were injected subcutaneously into the flanks of athymic nude mice (6-8 weeks). Visible tumors developed in approximately 2 weeks. Tumors were measured with electronic calipers and the tumor volume was calculated according to the formula $V = 0.52 \times L \times W^2$. Mice with established tumors were randomized to drug treatment groups: AZD6244 25 mg/kg (0.5% methylcellulose/0.4% polysorbate), GDC-0941 100 mg/kg (0.5% methylcellulose/0.2% Tween-80), ABT-263 100 mg/kg (30% PEG400/60% Phosal 50 PG/10% ethanol), or combinations. Drug treatments were administered by oral gavage. *Kras* and *Kras* $p53^{L/L}$ mouse strains harboring a conditional activating mutation (G12D) at the endogenous *Kras* locus, and conditional *Trp53* knockout were described previously (22). Tumor burden was quantified by serial MRI scanning as described (23). MEKi/PI3Ki treatments included AZD6244 (25 mg/kg) once daily combined either GDC-0941 (150 mg/kg), BEZ235 (50 mg/kg) or BKM120 (50 mg/kg) once daily. For pharmacodynamic studies, mice were sacrificed and tumors removed 3 hours after drug administration on day 3. Tumors were divided and snap frozen or formalin fixed.

Data and statistical analysis

Data were analyzed using GraphPad Prism software (GraphPad Software). Western blot band quantitation was performed using SynGene Gene Tools Software. All correlation calculations were carried out using the Spearman's correlation test. Comparisons between groups (e.g., experimental versus control) were made using paired or unpaired T-tests as appropriate. *P* values below 0.05 were considered to be statistically significant and are indicated by asterisks unless otherwise noted.

Results

KRAS mutant NSCLC cell lines have highly variable apoptotic response to MEKi/PI3Ki

Our earlier studies suggested that the responses to MEKi/PI3Ki in genetically engineered mouse *Kras* mutant NSCLC models can be variable, depending on the presence of concurrent secondary mutations (5, 24). For example, in these studies lung adenocarcinomas driven by mutant *Kras* in the absence of accompanying mutations had dramatic regressions (75% reduction in tumor burden) to combined treatment with the MEK inhibitor AZD6244 (selumetinib) and the dual PI3K/mTOR inhibitor NVP-BEZ235, whereas tumors with concurrent *Lkb1* deletion had minimal responses (20% reduction in tumor volume). We also examined the response of *Kras* mutant tumors with secondary *Trp53* deletion (22) to treatment with AZD6244/BEZ235 and observed a transient response of intermediate magnitude (60% reduction in tumor volume) that was followed by rapid development of drug resistance after four weeks (Figure S1). Similar responses were observed with AZD6244 in combination with the pan-PI3K inhibitors GDC-0941 or BKM120. These data indicate that the presence of secondary mutations can diminish the response of *KRAS* mutant NSCLC to combined MEKi/PI3Ki therapy, and suggest that significant heterogeneity of responsiveness may potentially exist among *KRAS* mutant lung cancers in the clinic.

Human *KRAS* mutant NSCLCs typically occur in the setting of tobacco smoke exposure and exhibit a high mutational burden (25). In contrast to the relative genetic simplicity of mouse models, cell lines derived from human tumors harbor multiple concurrent mutations or deletions in genes regulating growth and survival pathways (Table S1). To further model the response of human *KRAS* mutant NSCLC to MEKi/PI3Ki, we assessed the effects of AZD6244 in combination with GDC-0941 on cell proliferation, cell cycle progression and apoptosis using a panel of 20 human *KRAS* mutant NSCLC cell lines. MEKi/PI3Ki induced G1 arrest and reduced cell proliferation by 50-90% in all cell lines (Figure S2). Maximal inhibition of cell proliferation occurred with dual pathway inhibition (Figure S3). Treatment with AZD6244 alone increased AKT phosphorylation in several cell lines, underscoring the potential benefit of dual pathway inhibition in order to suppress activation of feedback signaling loops. Of note, the concentration of inhibitors chosen for use in subsequent studies was the lowest concentration that achieved >90% pathway inhibition.

Unexpectedly, we observed that the apoptotic response to MEKi/PI3Ki was highly variable despite the relatively uniform inhibition of cell cycle progression (Figure 1A, S4A-B). Only a minority of cell lines exhibited a robust apoptotic response similar to that of the *EGFR* mutant HCC827 NSCLC cell line treated with the EGFR inhibitor gefitinib (13, 26). Comparison of the effects of MEKi/PI3Ki on cell proliferation between low and high apoptosis cell lines revealed that cell lines with a minimal apoptotic response exhibited a net positive proliferative response in the presence of MEKi/PI3Ki, albeit reduced relative to vehicle treated cells (Figure 1B, S3D). In contrast, cell lines with a high apoptotic response had a net cytotoxic response to MEKi/PI3Ki, similar to HCC827 cells treated with gefitinib. Inhibiting apoptosis with the pan-caspase inhibitor QVD-Oph converted the cytotoxic response of A427 cells to a net proliferative response (Figure 1C, S4C), demonstrating the important contribution of apoptosis in addition to growth arrest for the in vitro effectiveness of MEKi/PI3Ki. Across the entire cell line panel, a cytotoxic response to MEKi/PI3Ki coincided with a high degree of both cell cycle arrest and apoptosis, and occurred only in a minority of cell lines (Figure 1D). Furthermore, *TP53* or *LKB1* mutational status did not correlate apoptotic responsiveness to MEKi/PI3Ki (Figure S5), though it is worth noting that the within each of these sub-groups, cell lines harbored varied additional mutations (Table S1).

To investigate the role of apoptosis in the response to MEKi/PI3Ki in vivo, we established xenograft tumors in mice from *KRAS* mutant cell lines with high (A427) or low (SW1573) apoptotic response. Prior to implantation, these cells were modified to express Gaussia luciferase, which is secreted into the blood allowing for precise quantitation of tumor cell viability (Reference (27) and Figure S6). Combination treatment of A427 xenografts with AZD6244/GDC-0941 resulted in decreased blood luciferase signal indicating decreased tumor cell viability, as well as increased cleaved caspase-3 immunostaining (Figure 1E-F). In contrast, combination treatment of SW1573 xenografts failed to activate caspase-3 and did not reduce blood luciferase signal despite comparable inhibition of both p-ERK and p-AKT (Figure S7). Taken together, these results suggest that failure to induce apoptosis may limit the efficacy of combined MEK and PI3K inhibition for *KRAS* mutant NSCLC in vitro and in vivo.

Variable apoptotic response is due to differential activation of mitochondrial apoptotic pathway

Tyrosine kinase signaling pathways modulate the mitochondrial pathway of apoptosis, which is regulated by the BCL-2 family proteins. MEKi/PI3Ki effectively suppressed the respective signaling pathways in cells with both high and low levels of apoptosis (Figure S3C, S8A), but only resulted in activation of BAX and cleavage of caspase-3 and PARP in cells undergoing apoptosis (Figure S8A-C).

To further assess if induction of apoptosis results from variability in the downstream inhibition of MEK and PI3K pathways, we examined transcriptional outputs following MEKi/PI3Ki treatment. mRNA levels of the MEK/ERK pathway targets *DUSP6*, *SPRY4* and *EGR-1* were dramatically reduced in all cell lines, regardless of degree of apoptotic response (Figure S9). Similarly, mRNA levels of the FOXO3a transcriptional targets *HER3* and *TRAIL* were induced in low and high apoptosis cell lines, consistent with comparable inhibition of PI3K/AKT. We also assessed whether differential activation of another RAS-effector pathway, RalGDS, which has been shown to play a role in RAS-induced tumorigenesis (28, 29), might contribute to the differential apoptotic response. However, pull-down assays of GTP-bound RAL-A, a small GTPase activated by RalGDS, revealed no clear differences in RAL-A activation in response to MEKi/PI3Ki between high and low apoptosis cell lines (Figure S10). In fact, a modest increase in GTP-bound RAL-A was observed following MEKi/PI3Ki in all three low apoptosis cell lines and two of three high apoptosis cell lines, possibly due to suppression of negative feedback loops. Additionally, there was no clear difference in baseline RAL-A activation between low and high apoptosis cell lines. This suggests that the differential apoptotic response induced by MEKi/PI3Ki is not simply explained by variable inhibition of RAS effector pathways, but may result from differential ability of the MEK and PI3K pathways to modulate the BCL-2 family of apoptotic regulatory proteins.

The apoptotic response to MEKi/PI3Ki in *KRAS* mutant NSCLC cell lines does not correlate with baseline mitochondrial apoptotic priming

Recently, the concept of mitochondrial priming has been proposed to explain the relative sensitivity of cancers to chemotherapeutic agents (30). In this paradigm, priming is a function of the proximity of a cell to the apoptotic threshold, determined by the collective expression of pro-versus anti-apoptotic BCL-2 family proteins. The extent of priming can be determined experimentally by BH3 profiling, which measures mitochondrial depolarization in response to exogenously added BH3 peptides that mimic the pro-apoptotic activity of BH3-only proteins including BIM, BID and PUMA (31, 32). To investigate whether the apoptotic response to MEKi/PI3Ki among *KRAS* mutant NSCLC cell lines is a function of mitochondrial priming, we performed BH3 profiling on five high and five low apoptosis cells. However, no correlation between baseline mitochondrial priming and apoptotic response to MEKi/PI3Ki was observed (Figure S11). This suggests that sensitivity of *KRAS* mutant NSCLC to MEKi/PI3Ki may be more dependent on dynamic changes in specific BCL-2 family proteins than overall baseline proximity to the apoptotic threshold, in contrast to what has been found for the less selective conventional cytotoxic chemotherapies (30).

PUMA, BIM and BCL-XL mediate the apoptotic response of *KRAS* mutant NSCLC cell lines to MEKi/PI3Ki

To determine the direct mediators of MEKi/PI3Ki-induced apoptosis, we performed a targeted shRNA screen of the BCL-2 family and assessed the impact on MEKi/PI3Ki-induced activation of caspase-3/7 in five high apoptosis *KRAS* mutant NSCLC cell lines (A427, DV-90, H2009, H1792 and A549). Each hairpin was verified to knock down expression of the target gene at the protein level (Table S2). In aggregate, knockdown of pro-apoptotic BH3-only proteins PUMA and BIM and the effector protein BAX led to reduced caspase-3/7 activation (Figure 2A). To confirm these results, we established cell lines with stable knockdown of BIM, PUMA, BAX and assessed the apoptotic response to MEKi/PI3Ki. Confirming the screen results, depletion of PUMA, BIM or BAX in A427 and A549 cells reduced caspase-3/7 activation in response to MEKi/PI3Ki compared to shGFP infected control cells (Figure 2B), and decreased the percentage of apoptotic cells (Figure 2C). Similar protection from apoptosis was observed after transfection with unrelated siRNAs targeting BIM, PUMA and BAX, reducing the likelihood that this effect is due to non-specific or off-target effects of the hairpins (Figure S12). This indicates that BIM and PUMA play a role in mediating the apoptotic response to MEKi/PI3Ki in *KRAS* mutant NSCLC cells.

As shown above, MEKi/PI3Ki failed to induce substantial apoptosis in many of the *KRAS* mutant NSCLC cell lines. To investigate whether anti-apoptotic BCL-2 family proteins play a role in mediating intrinsic resistance to MEKi/PI3Ki, we performed shRNA-mediated knockdown of BCL-XL, MCL-1, BCL-2, BCL-W and BFL-1/A1 in 10 low apoptosis *KRAS* mutant NSCLC cell lines. Knockdown of BCL-XL and MCL-1 alone resulted in increased basal apoptosis, and potentiated the apoptotic response to MEKi/PI3Ki (Figure 2D). Notably, knockdown of BCL-2 and other pro-survival BCl-2 family members failed to do so. Because gene knockdown of BCL-XL and MCL-1 led to substantially decreased viability and complicated the selection of cell lines with stable knockdown, we employed a pharmacologic strategy to confirm the hypothesis that anti-apoptotic BCL-2 family proteins such as BCL-XL contribute to resistance to MEKi/PI3Ki. In the majority of cell lines, the dual BCL-XL/BCL-2 inhibitor ABT-263 (navitoclax) stimulated a moderate degree of apoptosis, whereas a robust apoptotic response was observed after MEKi/PI3Ki treatment in the presence of ABT-263 (Figure 2E). Consistent with the shRNA results, this effect of ABT-263 was specific to inhibition of BCL-XL, as ABT-199, a selective BCL-2 inhibitor (33), showed no effect (Figure S13). Given the lack of a selective MCL-1 inhibitor, we were unable to similarly test the effect of MCL-1 inhibition on sensitivity to MEKi/PI3Ki. Nevertheless these results demonstrate that pro-survival BCL-2 family proteins such as BCL-XL protect some *KRAS* mutant NSCLC cells from MEKi/PI3Ki-induced apoptosis.

We next examined the effect of MEKi/PI3Ki on the expression of BCL-2 family proteins. Both PUMA and BIM protein accumulated after MEKi/PI3Ki treatment in both low and high apoptosis cells, whereas BCL-XL and MCL-1 levels were largely unchanged in the majority of cell lines (Figure S14A). The absolute expression levels of any of these BCL-2 family members alone (BIM, PUMA, BCL-XL or MCL-1) at baseline or after drug treatment did not correlate with apoptotic sensitivity. However, because apoptosis is

determined by the relative balance of pro- and anti-apoptotic BCL-2 family proteins, we also analyzed the collective expression levels of BIM and PUMA versus BCL-XL and MCL-1. Importantly, both at baseline and after drug treatment, the expression of BIM and PUMA protein levels relative to BCL-XL correlated highly with apoptotic response (Figure 2F), whereas accounting for the expression of MCL-1 did not improve the correlation (Figure S14B).

We previously reported that baseline mRNA expression levels of BIM could predict response to TKI treatment in *EGFR* mutant NSCLC (14). Because the relative fold accumulation of BIM protein after TKI treatment is similar among high and low apoptosis cancers, pre-treatment BIM mRNA levels effectively serve as a surrogate for on-treatment BIM levels. In an analogous manner, we observed that the difference in (BIM+PUMA)/BCL-XL ratios between high and low apoptosis cells was similar whether measured at baseline or after MEKi/PI3Ki treatment (2.3 and 2.2-fold, respectively; Figure S14C). Therefore, we examined whether pre-treatment mRNA levels of BIM and PUMA versus BCL-XL correlated with response to MEKi/PI3Ki. Across the entire panel of *KRAS* mutant NSCLC cell lines, the pretreatment ratio of BIM and PUMA relative to BCL-XL significantly correlated with apoptotic response to AZD644/GDC-0941 (Figure S14D). Taken together, these results indicate that the apoptotic response of *KRAS* mutant NSCLC to MEKi/PI3Ki is regulated by BIM, PUMA and BCL-XL, and suggest that differences in the relative expression of these proteins may underlie differential apoptotic sensitivity.

Restoration of apoptotic response sensitizes *KRAS* mutant NSCLC to MEKi/PI3Ki

To establish if decreased expression of pro-apoptotic relative to anti-apoptotic BCL-2 proteins underlies insensitivity to MEKi/PI3Ki, we tested whether altering the balance of BIM and BCLXL reversed the resistance of *KRAS* mutant NSCLC cell lines to MEKi/PI3Ki. First, we inducibly expressed BIM in low apoptosis H2030 and SW1573 cells. Ectopic expression of BIM restored the apoptotic response to MEKi/PI3Ki (Figure 3A, Figure S15) and resulted in a net cytotoxic response (Figure 3B). Second, we assessed the effects of BCL-XL inhibition on cell proliferation. Treatment of cells with ABT-263, which restores the apoptotic response to MEKi/PI3Ki (Figure 2E), likewise led to a cytotoxic response in the majority of insensitive cell lines (Figure 3C). In total, restoration of apoptosis either by increased expression of BIM or inhibition of BCL-XL correlated highly with conversion from a cytostatic to cytotoxic response to MEKi/PI3Ki across the panel of insensitive cell lines (Figure 3D). Finally, we examined if BCL-XL inhibition would translate to improved efficacy of MEKi/PI3Ki against insensitive *KRAS* mutant NSCLC in vivo. Consistent with the in vitro results, addition of ABT-263 to MEKi/PI3Ki led to regression of SW1573 xenograft tumors (Figure 3E, S16). Altogether, these results demonstrate that the inability for MEKi/PI3Ki to modulate BCL-2 family proteins sufficient to induce an apoptotic response contributes to intrinsic resistance of *KRAS* mutant NSCLC to MEKi/PI3Ki in vitro and in vivo.

Rapid adaptation of *KRAS* mutant NSCLC to MEKi/PI3Ki involves loss of apoptotic response

The clinical efficacy of targeted therapies is limited by the emergence of drug resistance (34). When studying the response of high apoptosis *KRAS* mutant NSCLC cell lines to MEKi/PI3Ki, we observed that cells that survived the initial exposure to drug were less sensitive on repeated drug exposure (Figure S17A). This suggests that even when cells are initially sensitive to MEKi/PI3Ki, efficacy might be limited by rapid adaptation to drug. To investigate whether suppression of apoptosis might underlie this adaptive response, we cultured A427 and DV-90 cells in the presence of AZD6244/GDC-0941 for 3 days followed by drug washout for 3 days (Figure S17B). Although initial drug treatment caused a robust apoptotic response, after five to ten intermittent drug treatments, the resulting resistant A427-R and DV-90-R cells no longer exhibited a cytotoxic response and were able to survive in the continuous presence of MEKi/PI3Ki (Figure 4A). MEKi/PI3Ki suppressed pERK, pAKT and pS6 as well as cell cycle progression in both resistant and parental cells (Figure 4B-C, S17C), indicating that resistance was not due to reactivation of these signaling pathways. In contrast, the resistant cells had a greatly diminished apoptotic response to MEKi/PI3Ki (Figure 4D, S17D), with decreased expression of BIM and PUMA (Figure 4B). Thus, loss of expression of pro-apoptotic BCL-2 family proteins leading to diminished apoptosis may underlie rapid adaptation of *KRAS* mutant NSCLC cancer to MEKi/PI3Ki.

To investigate whether suppression of apoptosis might contribute to rapid adaptation to MEKi/PI3Ki in vivo, we utilized the *Kras p53*$^{L/L}$ lung adenocarcinoma model. These tumors initially respond to MEKi/PI3Ki, but quickly develop resistance and progress after four weeks (Figure S1). We generated cell lines from *Kras p53*$^{L/L}$ tumors (R1, R2, R3) after progression on treatment with AZD6244/BEZ235, as well as from treatment naïve *Kras p53*$^{L/L}$ tumors (N1, N2) (Figure 5A, S18A,B). Cell lines from resistant tumors maintained resistance to MEKi/PI3Ki in vitro, with loss of the cytotoxic response exhibited by cell lines derived from treatment naïve tumors (Figure 5B). Importantly, resistant cell lines exhibited a significantly blunted apoptotic response to treatment with AZD6244/GDC-0941 (Figure 5C, S18C), despite undergoing cell cycle arrest (Figure S16D), similar to the differences observed between sensitive *KRAS* mutant NSCLC cell lines and those with intrinsic (Figure 1) or acquired (Figure 4) resistance.

We next examined whether differential expression of BCL-2 family proteins might be associated with resistance of *Kras p53*$^{L/L}$ tumors to MEKi/PI3Ki in vivo. For reasons unclear to us, analysis of BIM and PUMA protein expression from *Kras p53*$^{L/L}$ tumors yielded variable and inconsistent results. Thus, we investigated whether mRNA levels of BCL-2 family proteins correlated with apoptotic responsiveness of cell lines derived from *Kras p53*$^{L/L}$ tumors, as we observed with the human *KRAS* NSCLC cell lines described above. Compared to cells derived from treatment naïve tumors, those derived from resistant tumors exhibited significantly decreased BIM mRNA expression, whereas PUMA and BCL-XL levels were similar (Figure 5D, S19). Notably, the pretreatment ratio of BIM relative to BCL-XL correlated with apoptotic response and was diminished in cells from resistant tumors (Figure 5E). Finally, we examined whether pharmacologic inhibition of BCL-XL with ABT-263 could resensitize resistant tumor cell lines to MEKi/PI3Ki. Treatment of

resistant *Kras p53*$^{L/L}$ cells with AZD6244/GDC0941 in the presence of 100 nM of ABT-263 led to equivalent apoptosis as treatment naïve cells with MEKi/PI3Ki alone (Figure 5G). Altogether, these data indicate that a diminished apoptotic response associated with loss of expression of pro-apoptotic BCL-2 family proteins may result in rapid adaptation of *KRAS* mutant NSCLC to MEKi/PI3Ki in vitro and in vivo.

Discussion

There is increasing evidence that differences in the apoptotic response amongst cancers with the same primary oncogenic driver may result in variable clinical responses to targeted therapies (14, 15). In this study, we find that differences in the apoptotic response contribute to variable in vitro and in vivo responsiveness of *KRAS* mutant NSCLC experimental models to combined MEK and PI3K inhibition, a therapeutic combination currently being investigated in the clinic. Although emerging data from clinical studies indicates significant activity in *KRAS* mutant ovarian cancers and some lung cancers, the activity in *KRAS* mutant NSCLC in general has been underwhelming (9, 12, 35). While clinical efficacy may be limited by issues related to dosing and toxicity, our data may explain why the effectiveness of MEKi/PI3Ki may be limited, even when full suppression of the signaling pathways can be achieved. Since a large subset of *KRAS* mutant lung cancers may be relatively insensitive MEKi/PI3Ki even with optimal inhibition, the findings in this study may become even more salient as innovative therapeutic dosing strategies are developed.

The extent to which secondary mutations affect response to targeted therapies is incompletely understood. Initial studies demonstrating impressive activity of MEKi/PI3Ki utilized genetically engineered mouse models of *KRAS* mutant NSCLC with no additional mutations (5). Subsequent studies utilizing tumors with concomitant deletion of *Trp53* or *Lkb1* have shown less impressive responses of these mouse models to targeted therapies including MEKi/PI3Ki (23, 24). However, there remains limited data on the impact of secondary mutations on clinical response to targeted therapies in patients. This may be especially relevant to *KRAS* mutant lung cancers, which are associated with a history of cigarette smoking and exhibit increased mutational burden (25). In this study, we modeled the heterogeneity of human NSCLC by employing a large panel of *KRAS* mutant NSCLC cell lines that harbor numerous and diverse secondary mutations in key growth and survival pathways (Table S1). Using these models, MEKi/PI3Ki demonstrated much less impressive activity than the original mouse studies with *Kras* mutations alone, more akin to what is being observed in the clinic. Despite induction of cell cycle arrest across the panel of cell lines, MEKi/PI3Ki was largely ineffective at provoking sufficient apoptosis to cause a cytotoxic response in the majority of cell lines. In contrast to the genetically engineered mouse models, we did not observe statistically significant correlations between apoptotic response and TP53 or LKB1 mutational status. The reasons for this are unclear, however it is possible that additional mutations present in the cell lines modify the responses to MEKi/PI3Ki. It is worth noting that all but one (A427) LKB1 mutant cell line exhibited low levels of apoptosis, consistent with the lack of response to MEKi/PI3Ki observed in the *Kras Lkb1* mice (24). However, these studies point to the potential limitation of genetically engineered mouse models for predicting response to novel therapeutic combinations.

While our study adds to the growing evidence for the importance of the apoptotic response for effective targeted therapies, it also suggests that loss of the apoptotic response secondary to down-regulation of pro-apoptotic mediators may contribute to adaptive or acquired resistance to targeted therapies. This may be especially relevant to therapies that inhibit downstream effector signaling pathways such as MEK and PI3K rather than a receptor tyrosine kinase (e.g., mutant EGFR), because resistance to receptor tyrosine kinase inhibitors can be achieved by mutations in the receptor (e.g., EGFR T790M) or activation of alternate pathways (i.e., bypass tracks) that lead to re-activation of downstream signaling nodes such as MEK and PI3K (26, 36, 37). In contrast, *KRAS* mutant NSCLC cell lines with acquired resistance to MEKi/PI3Ki still exhibited suppression of MEK/ERK and PI3K/AKT signaling and cell cycle arrest upon drug treatment, but this failed to translate into an apoptotic response. Thus strategies to overcome either intrinsic or adaptive resistance may need to focus specifically on restoration of the apoptotic response, such as use of epigenetic regulators to increase transcription of pro-apoptotic proteins or direct targeting of anti-apoptotic BCL-2 family members (15, 38). As proof of concept, we demonstrate that restoration of BIM expression or use of ABT-263 can re-sensitize resistant *KRAS* mutant human and mouse cancer cells, respectively, to MEKi/PI3Ki.

In summary, we feel that this study has important implications for the use of combined MEK and PI3K inhibitors and other targeted therapies for the treatment of *KRAS* mutant NSCLC. While MEKi/PI3Ki may be effective for some *KRAS* mutant cancers, it is unlikely to be universally effective given the heterogeneity observed among human *KRAS* mutant lung cancers. Future investigations of novel therapies for *KRAS* mutant NSCLC should account for this heterogeneity in order to maximize potential for clinical success. Additionally, the development of biomarkers beyond the primary oncogenic driver will likely be crucial for predicting which patients will respond to specific therapies. For example, apoptotic biomarkers combined with standard genotyping may be useful in predicting response to targeted therapies (14). Finally, given the importance of the apoptotic response, combination therapies that directly target BCL-2 family proteins may be a useful component of therapeutic strategies for *KRAS* mutant cancers (39).

Supplementary Material

Refer to Web version on PubMed Central for supplementary material.

Acknowledgments

We thank Sylvie Roberge and Euihon Chung (MGH) for assistance with in vivo Gluc experiments. We thank the AACR/SU2C PI3K Dream Team for supplying GDC-0941 for in vivo studies.

Grant Support NIH R01CA137008-01 (JAE), R01CA140594 (JAE/KKW), 1U01CA141457-01 (JAE), R01CA122794 (KKW), R01CA137181 (KKW), 1RC2CA147940 (KKW), NCI Lung SPORE P50CA090578 (JAE/KKW), V Foundation Translational Research Grant (JAE), American Cancer Society RSG-06-102-01-CCE (JAE), Ellison Foundation Scholar Award (JAE), American Lung Cancer Association Lung Cancer Discover Award (JAE), Uniting Against Lung Cancer Foundation (KKW), and the Susan Spooner Research Fund (KKW).

References

1. Maemondo M, Inoue A, Kobayashi K, Sugawara S, Oizumi S, Isobe H, et al. Gefitinib or chemotherapy for non-small-cell lung cancer with mutated EGFR. N Engl J Med. 2010; 362(25): 2380–8. [PubMed: 20573926]
2. Mitsudomi T, Morita S, Yatabe Y, Negoro S, Okamoto I, Tsurutani J, et al. Gefitinib versus cisplatin plus docetaxel in patients with non-small-cell lung cancer harbouring mutations of the epidermal growth factor receptor (WJTOG3405): an open label, randomised phase 3 trial. Lancet Oncol. 2010; 11(2):121–8. [PubMed: 20022809]
3. Kwak EL, Bang Y-J, Camidge DR, Shaw AT, Solomon B, Maki RG, et al. Anaplastic Lymphoma Kinase Inhibition in Non‐Small-Cell Lung Cancer. New England Journal of Medicine. 2010; 363(18):1693–703. [PubMed: 20979469]
4. Young A, Lyons J, Miller AL, Phan VT, Alarcon IR, McCormick F. Ras signaling and therapies. Advances in cancer research. 2009; 102:1–17. [PubMed: 19595305]
5. Engelman JA, Chen L, Tan X, Crosby K, Guimaraes AR, Upadhyay R, et al. Effective use of PI3K and MEK inhibitors to treat mutant Kras G12D and PIK3CA H1047R murine lung cancers. Nat Med. 2008; 14(12):1351–6. [PubMed: 19029981]
6. She QB, Halilovic E, Ye Q, Zhen W, Shirasawa S, Sasazuki T, et al. 4E-BP1 is a key effector of the oncogenic activation of the AKT and ERK signaling pathways that integrates their function in tumors. Cancer Cell. 2010; 18(1):39–51. [PubMed: 20609351]
7. Sos ML, Fischer S, Ullrich R, Peifer M, Heuckmann JM, Koker M, et al. Identifying genotype-dependent efficacy of single and combined PI3K- and MAPK-pathway inhibition in cancer. Proc Natl Acad Sci U S A. 2009; 106(43):18351–6. [PubMed: 19805051]
8. Kinross KM, Brown DV, Kleinschmidt M, Jackson S, Christensen J, Cullinane C, et al. In Vivo Activity of Combined PI3K/mTOR and MEK Inhibition in a KrasG12D;Pten Deletion Mouse Model of Ovarian Cancer. Mol Cancer Ther. 2011; 10(8):1440–9. [PubMed: 21632463]
9. Bedard, P.; Tabernero, J.; Kurzrock, R.; Britten, CD.; Stathis, A.; Perez-Garcia, JM., et al., editors. A phase lb, open-label, multicenter, dose-escalation study of the oral pan-PI3K inhibitor BKM120 in combination with the oral MEK1/2 inhibitor GSK1120212 in patients (pts) with selected advanced solid tumors. ASCO Annual Meeting; Chicago IL. 2012.
10. Infante, JR.; Gandhi, L.; Shapiro, G.; Burris, HA.; Bendell, JC.; Baselga, J., et al., editors. Phase lb combination trial of a MEK inhibitor, pimasertib (MSC1936369B), and a PI3K/mTOR inhibitor, SAR245409, in patients with locally advanced or metastatic solid tumors. ASCO Annual Meeting; Chicago IL. 2012.
11. LoRusso, P.; Shapiro, G.; Pandya, SS.; Kwak, EL.; Jones, C.; Belvin, M., et al., editors. A first-in-human phase Ib study to evaluate the MEK inhibitor GDC-0973, combined with the pan-PI3K inhibitor GDC-0941, in patients with advanced solid tumors. ASCO Annual Meeting; Chicago IL. 2012.
12. Infante, JR.; Gandi, L.; Shapiro, G.; Rizvi, N.; Howard, A.; Burris, I.; Bendell, JC., et al., editors. Combination of the MEK inhibitor, pimasertib (MSC1936369B), and the PI3K/mTOR inhibitor, SAR245409, in patients with advanced solid tumors: Results of a phase Ib dose-escalation trial. AACR Annual Meeting; Washington DC. 2013.
13. Faber AC, Li D, Song Y, Liang MC, Yeap BY, Bronson RT, et al. Differential induction of apoptosis in HER2 and EGFR addicted cancers following PI3K inhibition. Proc Natl Acad Sci U S A. 2009; 106(46):19503–8. [PubMed: 19850869]
14. Faber AC, Corcoran RB, Ebi H, Sequist LV, Waltman BA, Chung E, et al. BIM expression in treatment naïve cancers predicts responsiveness to kinase inhibitors. Cancer Discov. 2011; 1(4): 352–65. [PubMed: 22145099]
15. Ng KP, Hillmer AM, Chuah CT, Juan WC, Ko TK, Teo AS, et al. A common BIM deletion polymorphism mediates intrinsic resistance and inferior responses to tyrosine kinase inhibitors in cancer. Nat Med. 2012; 18(4):521–8. [PubMed: 22426421]
16. Luciano F, Jacquel A, Colosetti P, Herrant M, Cagnol S, Pages G, et al. Phosphorylation of Bim-EL by Erk1/2 on serine 69 promotes its degradation via the proteasome pathway and regulates its proapoptotic function. Oncogene. 2003; 22(43):6785–93. [PubMed: 14555991]

17. Cragg MS, Kuroda J, Puthalakath H, Huang DC, Strasser A. Gefitinib-induced killing of NSCLC cell lines expressing mutant EGFR requires BIM and can be enhanced by BH3 mimetics. PLoS Med. 2007; 4(10):1681–89. [PubMed: 17973573]

18. Costa DB, Halmos B, Kumar A, Schumer ST, Huberman MS, Boggon TJ, et al. BIM mediates EGFR tyrosine kinase inhibitor-induced apoptosis in lung cancers with oncogenic EGFR mutations. PLoS Med. 2007; 4(10):1669–79. [PubMed: 17973572]

19. Gong Y, Somwar R, Politi K, Balak M, Chmielecki J, Jiang X, et al. Induction of BIM is essential for apoptosis triggered by EGFR kinase inhibitors in mutant EGFR-dependent lung adenocarcinomas. PLoS Med. 2007; 4(10):1655–68.

20. Barbie DA, Tamayo P, Boehm JS, Kim SY, Moody SE, Dunn IF, et al. Systematic RNA interference reveals that oncogenic KRAS-driven cancers require TBK1. Nature. 2009; 462(7269): 108–12. [PubMed: 19847166]

21. Garnett MJ, Edelman EJ, Heidorn SJ, Greenman CD, Dastur A, Lau KW, et al. Systematic identification of genomic markers of drug sensitivity in cancer cells. Nature. 2012; 483(7391): 570–5. [PubMed: 22460902]

22. Ji H, Ramsey MR, Hayes DN, Fan C, McNamara K, Kozlowski P, et al. LKB1 modulates lung cancer differentiation and metastasis. Nature. 2007; 448(7155):807–10. [PubMed: 17676035]

23. Chen Z, Cheng K, Walton Z, Wang Y, Ebi H, Shimamura T, et al. A murine lung cancer co-clinical trial identifies genetic modifiers of therapeutic response. Nature. 2012; 483(7391):613–7. [PubMed: 22425996]

24. Carretero J, Shimamura T, Rikova K, Jackson AL, Wilkerson MD, Borgman CL, et al. Integrative genomic and proteomic analyses identify targets for Lkb1-deficient metastatic lung tumors. Cancer Cell. 2010; 17(6):547–59. [PubMed: 20541700]

25. Govindan R, Ding L, Griffith M, Subramanian J, Dees ND, Kanchi KL, et al. Genomic landscape of non-small cell lung cancer in smokers and never-smokers. Cell. 2012; 150(6):1121–34. [PubMed: 22980976]

26. Engelman JA, Zejnullahu K, Mitsudomi T, Song Y, Hyland C, Park JO, et al. MET amplification leads to gefitinib resistance in lung cancer by activating ERBB3 signaling. Science. 2007; 316(5827):1039–43. [PubMed: 17463250]

27. Chung E, Yamashita H, Au P, Tannous BA, Fukumura D, Jain RK. Secreted Gaussia luciferase as a biomarker for monitoring tumor progression and treatment response of systemic metastases. PLoS One. 2009; 4(12):1–8.

28. Lim KH, Baines AT, Fiordalisi JJ, Shipitsin M, Feig LA, Cox AD, et al. Activation of RalA is critical for Ras-induced tumorigenesis of human cells. Cancer Cell. 2005; 7(6):533–45. [PubMed: 15950903]

29. Martin TD, Samuel JC, Routh ED, Der CJ, Yeh JJ. Activation and involvement of Ral GTPases in colorectal cancer. Cancer Res. 2011; 71(1):206–15. [PubMed: 21199803]

30. Ni Chonghaile T, Sarosiek KA, Vo TT, Ryan JA, Tammareddi A, Moore Vdel G, et al. Pretreatment mitochondrial priming correlates with clinical response to cytotoxic chemotherapy. Science. 2011; 334(6059):1129–33. [PubMed: 22033517]

31. Certo M, Del Gaizo, Moore V, Nishino M, Wei G, Korsmeyer S, Armstrong SA, et al. Mitochondria primed by death signals determine cellular addiction to antiapoptotic BCL-2 family members. Cancer Cell. 2006; 9(5):351–65. [PubMed: 16697956]

32. Deng J, Carlson N, Takeyama K, Dal Cin P, Shipp M, Letai A. BH3 profiling identifies three distinct classes of apoptotic blocks to predict response to ABT-737 and conventional chemotherapeutic agents. Cancer Cell. 2007; 12(2):171–85. [PubMed: 17692808]

33. Souers AJ, Leverson JD, Boghaert ER, Ackler SL, Catron ND, Chen J, et al. ABT-199, a potent and selective BCL-2 inhibitor, achieves antitumor activity while sparing platelets. Nat Med. 2013; 19(2):202–8. [PubMed: 23291630]

34. Sequist LV, Waltman BA, Dias-Santagata D, Digumarthy S, Turke AB, Fidias P, et al. Genotypic and histological evolution of lung cancers acquiring resistance to EGFR inhibitors. Science translational medicine. 2011; 3(75):75ra26.

35. Khan, KH.; Yan, L.; Mezynski, J.; Patnaik, A.; Moreno, V.; Papadopoulos, KP., et al., editors. A phase I dose escalation study of oral MK-2206 (allosteric Akt inhibitor) with oral selumetinib

(AZD6244; ARRY-142866) (MEK 1/2 inhibitor) in patients with advanced or metastatic solid tumors. ASCO Annual Meeting; Chicago IL. 2012.

36. Katayama R, Shaw AT, Khan TM, Mino-Kenudson M, Solomon BJ, Halmos B, et al. Mechanisms of acquired crizotinib resistance in ALK-rearranged lung Cancers. Science translational medicine. 2012; 4(120):120ra17.
37. Wilson TR, Fridlyand J, Yan Y, Penuel E, Burton L, Chan E, et al. Widespread potential for growth-factor-driven resistance to anticancer kinase inhibitors. Nature. 2012; 487(7408):505–9. [PubMed: 22763448]
38. Chen S, Dai Y, Pei XY, Grant S. Bim upregulation by histone deacetylase inhibitors mediates interactions with the Bcl-2 antagonist ABT-737: evidence for distinct roles for Bcl-2, Bcl-xL, and Mcl-1. Molecular and cellular biology. 2009; 29(23):6149–69. [PubMed: 19805519]
39. Corcoran RB, Cheng KA, Hata AN, Faber AC, Ebi H, Coffee EM, et al. Synthetic Lethal Interaction of Combined BCL-XL and MEK Inhibition Promotes Tumor Regressions in KRAS Mutant Cancer Models. Cancer Cell. 2013; 23(1):121–8. [PubMed: 23245996]

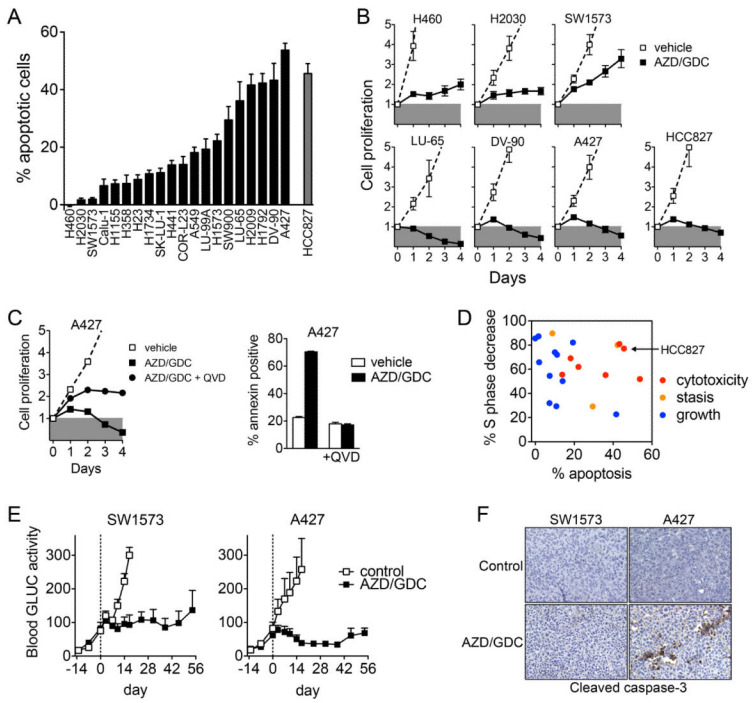

Figure 1. Apoptosis is necessary for tumor regression in response to MEKi/PI3Ki in vitro and in vivo

A. Cells were treated with 1 μM AZD6244/GDC-0941 or 1 μM gefitinib (HCC827) and the apoptotic response was determined by annexin staining and flow cytometry. % apoptotic cells were determined by subtracting annexin positive cells with vehicle treatment. Data are mean and standard error of 4-8 independent experiments.

B. Cells were treated 1 μM AZD6244/GDC-0941 or 1 μM gefitinib (HCC827, closed squares) and cell proliferation determined by CellTiter-Glo viability assay. Data are normalized to baseline value at the time of initial drug treatment (day 0) and are mean and standard error of three independent experiments.

C. Cells were treated with AZD6244/GDC-0941 with or without 20 μM QVD-Oph. Data shown are mean and standard error of triplicate samples.

D. Apoptosis and cell cycle arrest are necessary for cytotoxic response of *KRAS* mutant NSCLC to MEKi/PI3Ki. Each data point represents a different cell line. The response of the *EGFR* mutant HCC827 cells to gefitinib is shown for comparison. Data combined from Figures 1A, 1B, S2A.

E. Mice bearing SW1573-GLUC and A427-GLUC subcutaneous xenografts were treated with 100 mg/kg GDC-0941 plus 25 mg/kg AZD6244 once daily by oral gavage and secreted luciferase in whole blood was measured. Data shown are mean and standard error (SW1573: control n=4, AZD/GDC n=4; A427: control n=4, AZD/GDC n=5).

F. A427 but not SW1573 xenograft tumors have increased caspase-3 activation following short term MEKi/PI3Ki treatment.

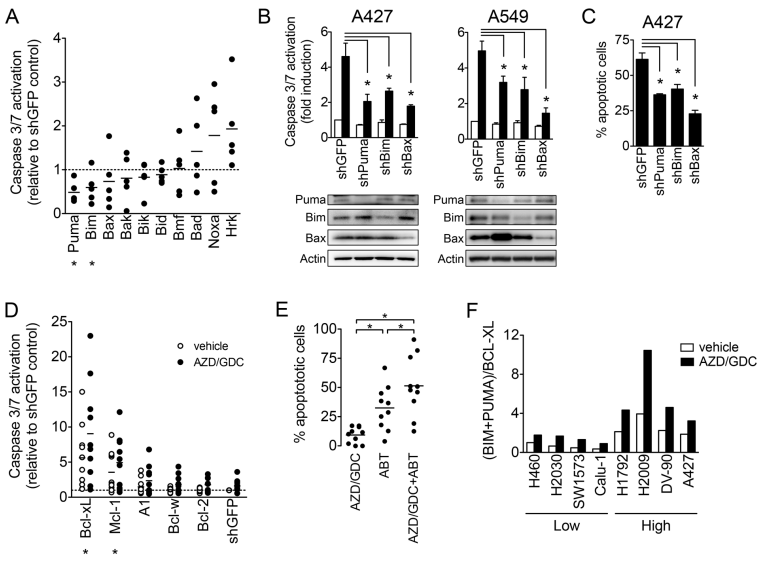

Figure 2. PUMA, BIM and BCL-XL mediate the apoptotic response to MEKi/PI3Ki

A. Five sensitive cells lines (A427, DV-90, H2009, H1792, A549) were infected with lentivirus harboring shRNA targeting pro-apoptotic BCL-2 family. Caspase-3/7 activity was determined 48 hours after treatment with 1 μM AZD6244/GDC-0941. Each data point represents the mean caspase activation of an individual cell line (2-5 independent replicates) relative to shGFP control. Asterisks indicate significant difference ($p<0.05$) compared to shGFP control.

B. Caspase 3/7 activation following treatment with 1 μM AZD6244/GDC-0941 was determined for cell lines with stable knockdown of the indicated BCL-2 family. Data shown are mean and standard error of 3-4 independent experiments.

C. Apoptotic cells (annexin positive) were determined after treatment with 1 μM AZD6244/GDC-0941.

D. Ten insensitive cell lines (H460, H2030, SW1573, H1155, H358, H23, Calu-1, CORL-23, SK-LU-1, H1734, H1155) were infected with lentivirus harboring shRNAs targeting pro-survival BCL-2 family members followed by treatment with 1 μM AZD6244/GDC-0941. Each data point represents the mean relative caspase activation of an individual cell line (2-5 independent replicates) compared to shGFP vehicle control.

E. Cell lines were treated with 1 μM AZD6244, GDC-0941, ABT263 or combination. Each symbol represents the mean (3-4 independent experiments) for a single cell line.

F. Cell lines were treated with 1 μM AZD6244/GDC-0941 or vehicle for 24 hours and protein expression levels were quantified from western blots and normalized to vehicle treated H460 cells. For representative western blot see Figure S14A. Data are the mean of three independent experiments.

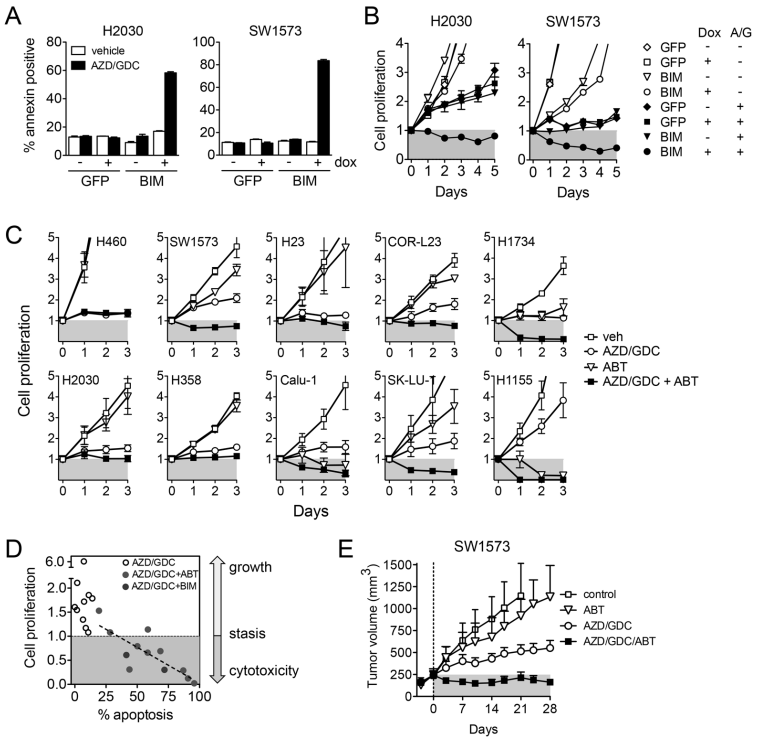

Figure 3. Induction of apoptosis restores responsiveness of insensitive *KRAS* mutant NSCLC cell lines and leads to tumor regression in vivo

A. Cells expressing BIM or GFP under control of a tetracycline inducible promoter (pTREX) were treated with doxycycline and 1 μM AZD6244/GDC-0941 as indicated and apoptosis determined.

B. Cells were treated with doxycycline and AZD6244/GDC-0941 and cell proliferation determined. Data shown are mean and standard error of triplicate samples and are representative of three independent experiments.

C. Cell lines were treated with 1 μM AZD6244, GDC-0941, ABT-263 or combination. Data are mean and standard error of three independent experiments.

D. Restoration of apoptotic response by BIM expression (Figure 3A,B) or BCL-XL inhibition by ABT263 (Figure 2E, 3C) correlates with conversion of cytostatic to cytotoxic response to MEKi/PI3Ki in insensitive *KRAS* mutant NSCLC cells.

E. Mice bearing SW1573 xenografts were treated with vehicle control, 25 mg/kg AZD6244, 100 mg/kg GDC-0941, 100 mg/kg ABT-263 or combination once daily by oral gavage (n=4 per group). Data shown are mean and standard error.

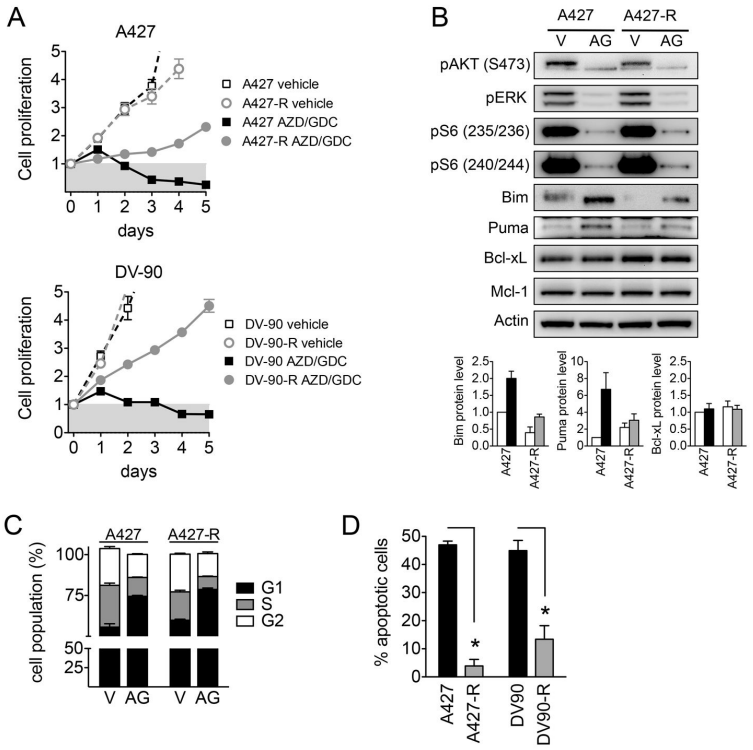

Figure 4. Loss of apoptotic response underlies adaptive resistance to MEKi/PI3Ki in vitro

A. Resistant (A427-R and DV-90-R) and parental cells were treated with 1 μM AZD6244/GDC-0941 and cell proliferation measured.

B. A427 and A427-R cells were treated with 1 μM AZD6244/GDC-0941 (AG) or vehicle (V) for 24 hours. Lower: Quantitation of protein expression from western blots. Data are mean and error of three independent experiments.

C. Cells were treated with 1 μM AZD6244/GDC-0941 for 24 hours, stained with propidium iodide and cell cycle populations analyzed by flow cytometry.

D. Cells were treated with 1 μM AZD6244/GDC-0941 and apoptosis determined by annexin staining. Data shown are mean and standard error of 5-7 independent experiments.

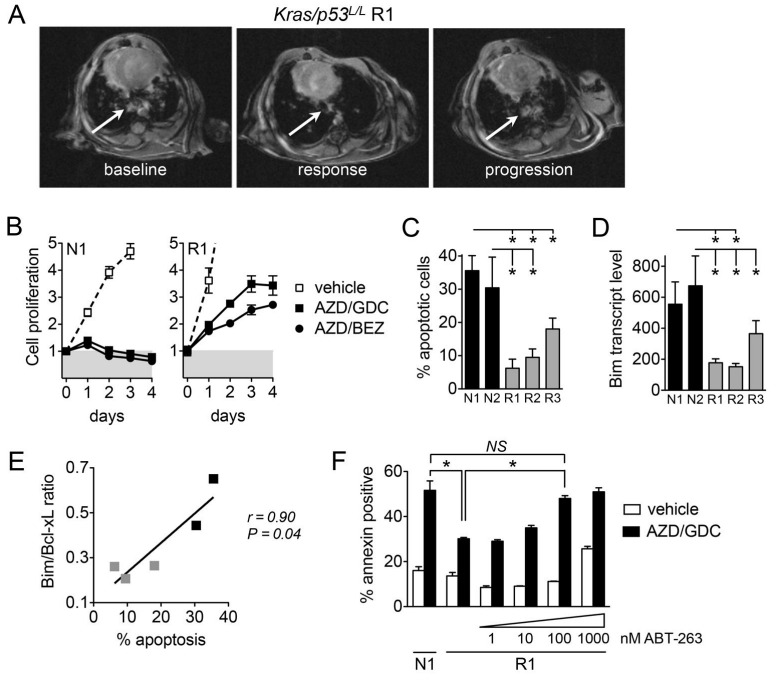

Figure 5. Loss of apoptotic response underlies acquired resistance to MEKi/PI3Ki in vivo

A. Cell lines established from resistant *Kras p53*$^{L/L}$ tumors after progression during MEKi/PI3Ki treatment. MRI images of R1 tumor nodule (arrow) at baseline, after treatment with AZD6244/BEZ235 (response, -72% change from baseline), and on-treatment progression (resistant, +200% change from nadir).

B. Cell lines derived from treatment naïve (N1) and resistant (R1) tumor nodules were treated with 1 μM AZD6244/GDC-0941 or 1 μM AZD6244/BEZ235.

C. Cell lines from resistant *Kras p53*$^{L/L}$ tumors (R1, R2, R3) and treatment naïve tumors (N1, N2) were treated with 1 μM AZD6244/GDC-0941 and apoptosis determined by annexin staining. Data shown are the mean and standard error of 3-4 independent experiments.

D. BIM mRNA expression levels were determined by quantitative RT-PCR. Data shown are mean and error of 3 independent experiments.

E. Correlation of BIM/BCL-XL ratios with apoptotic response for resistant (gray) and naïve (black) tumor derived cell lines.

F. Cell lines were treated with AZD6244/GDC-0941 with or without ABT-263 and apoptosis determined. Data shown are mean and error of triplicate samples.